*Proc. of the 8th International Symposium on Geotechnical Safety and Risk (ISGSR)*
*Edited by* Jinsong Huang, D.V. Griffiths, Shui-Hua Jiang, Anna Giacomini and Richard Kelly
 *Published by* Research Publishing, Singapore.
doi: 10.3850/978-981-18-5182-7_00-006-cd



# Geotechnical Probability: From FOSM to RFEM

D. V. Griffiths[1]

[1]Department of Civil and Environmental Engineering,
Colorado School of Mines, Golden, CO, USA.
E-mail: d.v.griffiths@mines.edu

**Abstract:**For geotechnical professionals, the words "risk" and "probability" should not be confused, since risk is the probability of design failure weighted by its consequences. An obvious implication of this definition is that if the consequences of a failure are serious in terms of loss of life and/or cost to infrastructure, the allowable or target probability of failure for design must be commensurately low. Conversely, if the consequences of failure are relatively less important, a higher allowable or target probability for design can be allowed. Risk is therefore inextricably linked to quantitative probability estimates. Geotechnical engineers have a toolbox of methods available for estimating probability, ranging from hand calculation methods such as the First Order Second Moment (FOSM) method, to mildly computational method such as the First Order Reliability Method (FORM) to intensively computational numerical methods such as the Random Finite Element Method (RFEM). This paper reviews these methods, offers an alternative approach to FORM, and highlights some of their characteristics that can be taken into account when applying them to probabilistic geotechnical applications.

Keywords:Probability, Risk, First Order Methods, Monte-Carlo, Random Finite Element Methods

## 1 Introduction

In geotechnical design, Risk $(R)$ is defined as the Probability of Failure $(P)$ weighted by the Consequences of Failure $(C)$. The Probability of Failure is meant here in its broadest sense, ranging from actual failure (often catastrophic), for example of a dam or levee due to a flood or earthquake, to a more modest design (performance) failure,e.g. excessive differential settlement of a foundation due to settlement or swelling. Writing the above definition as

$$R = P \times C \tag{1}$$

and taking logs of both sides, we get

$$\log P = -\log R + \log C \tag{2}$$

which implies a linear relationship between $\log R$ and $\log P$.

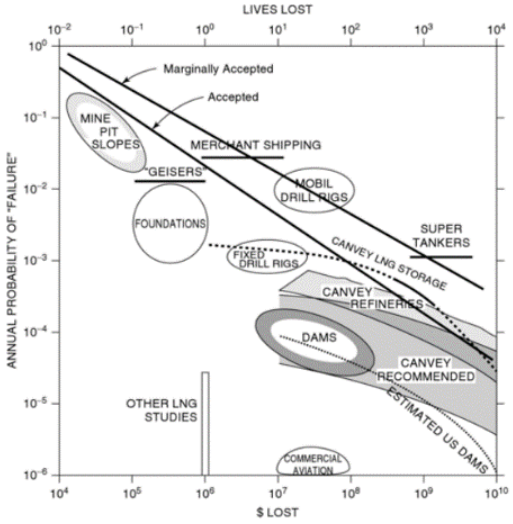


**Figure 1.** The Tonen FN Chart (T.W. Lambe & Associates 1982)

The implications of Eq. (2) were demonstrated graphically by Greg Baecher, with the collaboration of Allen Marr, while working on a seismic risk project involving a tank farm for the Tonen Oil Company of Japan (T.W. Lambe & Associates 1982). The resulting Figure 1 was never published in the academic press, but was presented as a personal communication by Whitman (1984), and later published in the text by Baecher and Christian

(2003)with further discussion by Baecher (2013). It has since been mimicked by numerous agencies involved with geotechnical risk

Consequences of failure are entirely site specific. In a deterministic analysis, the two failing slopes shown in Figure 2 have the same $FS = 1$, but quite different consequences of failure. In a risk analysis of the same two slopes, it would be justified in allowing a higher annual probability of failure of the slope on the left than for the slope to the right.

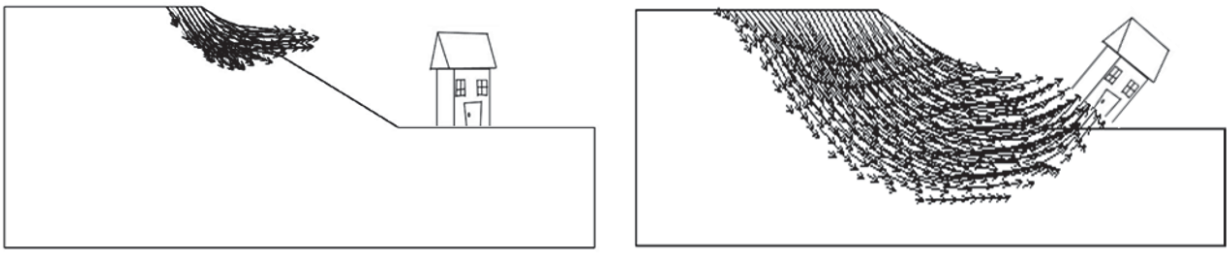

**Figure 2.** Two slopes with the same factor of safety but quite different consequences of failure

Geotechnical engineers have a choice of methods for estimating geotechnical probability, e.g.

1) Event Trees developed by Expert Panels
2) Point Estimate Methods (PEM)
3) First Order Methods
   i. First Order Second Moment (FOSM) Method
   ii. First Order Reliability Method (FORM)
4) Monte-Carlo Methods
   i. Single Random Variable (SRV) substitution.
   ii. Random Finite Element Method (RFEM)

A detailed description of most of these established methods can be found in the text by Baecher and Christian (2003) and Ang and Tang (2007). The relatively recent RFEM, developed by Griffiths and Fenton (1993), Fenton and Griffiths (1993), is now widely accepted as the state-of-the-art in probabilistic geotechnical analysis, and used by numerous research groups worldwide with a large and rapidly growing bibliography.

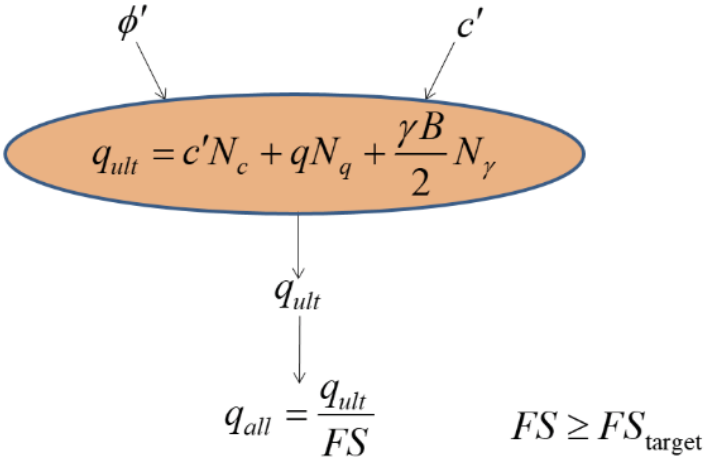


**Figure 3(a).** The traditional deterministic approach to a bearing capacity analysis

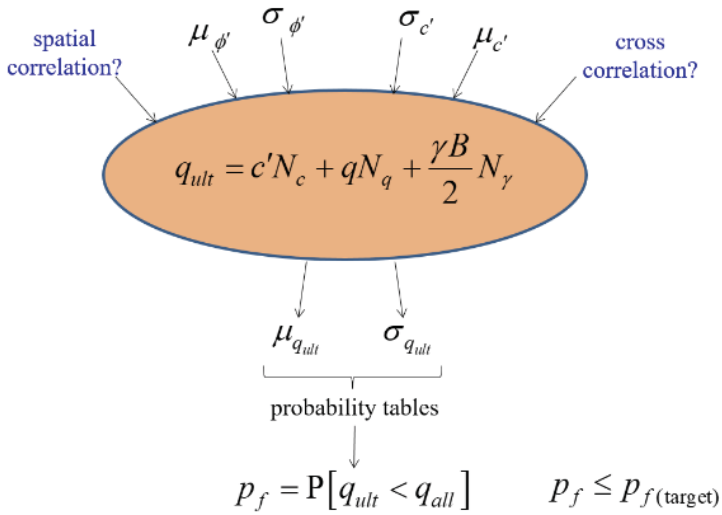


**Figure 3(b).** The probabilistic approach to a bearing capacity analysis

In the deterministic approach shown in Figure 3(a), the input parameters consist of characteristic values that typically represent pessimistic estimates of strength followed by application of the model (Terzaghi's bearing capacity equation in this case) and a Factor of Safety that must not fall below a design target value. If performance or serviceability governs design,characteristic values would then represent pessimistic estimates of soil compressibility. Although a characteristic value for a soil property represents a type of "mean", it takes no account of its variability.

The probabilistic approach shown in Figure 3(b) typically uses the same bearing capacity model, but instead of characteristic values, the input involves means and standard deviations of the key strength parameters. It is possible to include cross-correlation between parameters, and in a more advanced analysis such as that offered by RFEM, spatial correlation. The output delivered in this case would be the mean and standard deviation of the bearing capacity, from which probabilistic conclusions could be obtained using standard cumulative distribution tables. In this case, the analysis would wish to ensure that the probability of failure does not exceed some design target value. In the absence of quality data for the probabilistic input, presumptive values such as those shown in Table 1 (e.g.Lee et al. 1983, Duncan 2000, DiMaggio 2022) can be used as a starting point for parametric studies.

**Table 1.** Typical values of the Coefficient of Variation $\left(V = \sigma/\mu\right)$ for various soil properties

| Measured or interpreted parameter value | Coefficient of Variation, V (%) |
|---|---|
| Unit weight, $\gamma$ | 3 to 7 % |
| Buoyant unit weight, $\gamma_b$ | 0 to 10 % |
| Effective stress friction angle, $\phi'$ | 2 to 13 % |
| Undrained shear strength, $s_u$ | 13 to 40 % |
| Undrained strength ratio ($s_u/p_o$) | 5 to 15 % |
| Compression index, $C_c$ | 10 to 37 % |
| Preconsolidation pressure, $p_c$ | 10 to 35 % |
| Hydraulic conductivity of saturated clay, k | 68 to 90 % |
| Hydraulic conductivity of partially-saturated clay, k | 130 to 240 % |
| Coefficient of consolidation, $c_v$ | 33 to 68 % |
| Standard penetration blow count, N | 15 to 45 % |
| Electric cone penetration test, $q_c$ | 5 to 15 % |
| Mechanical cone penetration test, $q_c$ | 15 to 37 % |
| Vane shear test undrained strength, $s_{uVST}$ | 10 to 20 % |

In the remainder of this paper, the probabilities of failure of earth pressure and slope stability applications are estimated using First Order methods and RFEM. The aim of the discussion is to highlight some the characteristics of the methods that should be taken into account when applying them to probabilistic geotechnical applications.

## 2 FOSM

The First Order Second Moment Method (FOSM) is suitable for hand calculation of problems such as the one shown in Figure 3(b). Consider a "performance function" of $n$ random variables given as $f\left(X_1, X_2, \ldots, X_n\right)$, where the random variables have estimated means and standard deviations $\left(\mu_{X_1}, \sigma_{X_1}\right), \left(\mu_{X_2}, \sigma_{X_2}\right), \ldots, \left(\mu_{X_n}, \sigma_{X_n}\right)$. If the function is nonlinear, the FOSM method uses a truncated Taylor series to replace the function by a linear function in the vicinity of the mean (e.g. Ang and Tang 2007). The required *function* parameters are then estimated as:

$$\mu_f \approx f\left(\mu_{X_1}, \mu_{X_2}, \ldots \mu_{X_n}\right) \text{ and } \sigma_f \approx \sqrt{\sum_{i=1}^{n}\sum_{j=1}^{n}\left(\frac{\partial f}{dx_i}\right)\left(\frac{\partial f}{dx_j}\right)\mathrm{Cov}\left[X_i, X_j\right]} \tag{3}$$

The derivatives needed in Eq.(3) should be evaluated at the means and can be found either analytically or numerically. Numerical differentiation is used if analytical differentiation is inconvenient, or if no explicit function is available. The covariance terms are given as

$$\mathrm{Cov}\left[X_i, X_j\right] = \rho_{X_i X_j}\sigma_{X_i}\sigma_{X_j} \tag{4}$$

where $-1 \le \rho_{X_i X_j} \le 1$ is the dimensionless correlation coefficient between random variables $X_i$ and $X_j$.

Much has been made of the non-uniqueness of solutions given by FOSM,in that different arrangements of the performance function can lead to different function means, standard deviations, and ultimately different probabilistic estimates.

Consider a simple load ($L$) and resistance ($R$) analysis where $R$ and $L$ are uncorrelated random variables with parameters $\left(\mu_R, \sigma_R\right), \left(\mu_L, \sigma_L\right)$. Now consider a performance function $M = R - L$, where $M < 0$ implies failure and $M \ge 0$ implies safety. The quantity of interest in this problem is the probability of failure, i.e. $p_f = \mathrm{P}\left[M < 0\right]$. For illustration, let the load and resistance parameters be given as $\mu_L = 5,\ \sigma_L = 2$ and $\mu_R = 8,\ \sigma_R = 2\sqrt{2}$, and consider three arrangements of the performance function as shown in Table 2.

**Table 2.** Influence of function arrangement on $p_f$ in FOSM and FORM method

| | FOSM | FORM |
|---|---|---|
| Function | $p_f$ (%) | $p_f$ (%) |
| $M = R - L$ | 19.3 | 19.3 |
| $M = \frac{R}{L} - 1$ | 24.1 | 19.3 |
| $M = \ln\left(\frac{R}{L}\right)$ | 18.9 | 19.3 |

The problem has been solved using both the FOSM method and FORM (Hasofer and Lind 1974). The FOSM solution used Eqs.(3), and the FORM solution used a simple spreadsheet algorithm (e.g. Low and Tang 1997, 2007, Huang and Griffiths 2011)[1]. The table clearly shows the computed probabilities of failure by FOSM are different in each case, even though all the functional arrangements are mathematically equivalent. It is also noted that FORM gives the same result in all three cases.

The different probabilities in FOSM are caused by the differing gradients of the nonlinear performance function needed byEq.(3). The goal of the analysis is to find the closest failure point to the means, where the gradients are calculated. Only the first row in the table, namely the linear arrangement of the function achieves this exactly in FOSM (e.g. Baecher and Christian 2003). As noted by Schiermeyer (2009), the FOSM algorithm bears a striking resemblance to the Newton-Raphson method for solution of systems of nonlinear equations (e.g. Griffiths and Smith 2008) where the derivatives are used to "point" towards the solution corresponding to $M = f\left(X_1, X_2, \ldots, X_n\right) = 0$. The FOSM method is trying to find the solution in a single shot, i.e. just a single

[1] Excel FORM programs are available at the author's website: `https://inside.mines.edu/~vgriffit/FORM`

"iteration". If the equations to be solved are linear, Newton-Raphson obtains the exact solution in a single iteration, as does FOSM in a probabilistic study. Nonlinear arrangements of $M$ however, have derivatives at the mean point that do not point exactly at the solution, leading to different (incorrect) solutions when using just one iteration. Ang and Tang (2007) note that providing $M$ is not highly nonlinear, and the variances of the input random variables are relatively small, Eqs.(3) will give reasonable approximations.

FOSM has the benefit of being a hand calculation method that requires minimal computational help. It also involves calculation of derivatives, whose magnitudes and signs give useful physical insight into the sensitivity of the performance function to the various input parameters. Non-unique solutions remain a drawback of FOSM however, so users are strongly encouraged to seek a linear performance function when using FOSM, which will deliver the same probabilities as FORM.In spite of these drawbacks, FOSM is a useful introductory probabilistic tool for geotechnical analysis. It can give insight into geotechnical systems that are reasonably linear and with modest coefficients of variation of input variables. The following section shows a worked example of a geotechnical analysis using FOSM.

### 2.1 FOSM: Wall sliding example

The cantilever wall shown in Figure 4 retains a sand backfill and rests on a frictional base. The earth pressure is assumed to be at the limiting active state. The problem is similar to one presented by Duncan (2000), except with metric units and deterministic unit weights for the concrete $(\gamma_c)$and sand $(\gamma_{bf})$. The analysis includes two key probabilistic parameters, namely the Rankine active earth pressure coefficient ( $K_a$ ) and the coefficient of friction at the base of the wall (tanδ).

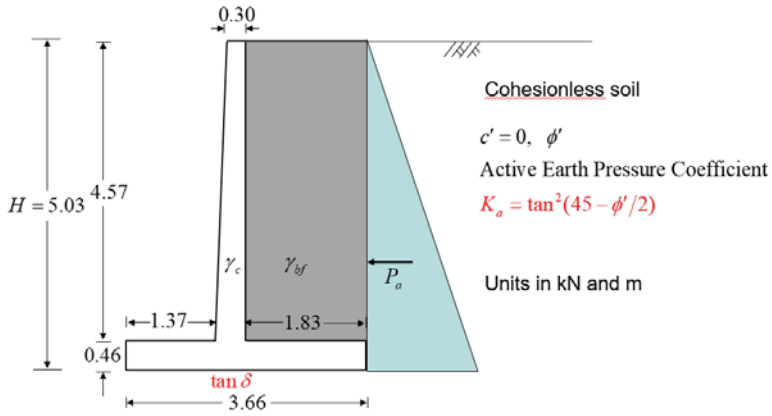


**Figure 4.** FOSM analysis of sliding of a cantilever retaining wall

The probabilistic input data are shown in Table 3, which initially includes some variability in the unit weights.

**Table 3.** Probabilistic input data for wall sliding problem

| Property | μ | σ |
|---|---|---|
| $\gamma_c$ (kN/m³) | 23.58 | 0.31 |
| $\gamma_{bf}$(kN/m³) | 18.87 | 1.10 |
| $K_a$ | 0.333 | 0.033 |
| tan δ | 0.5 | 0.05 |

The coefficient of variation of the unit weights are both small, as suggested by Table 1, so these parameters will betreated as deterministic and fixed at their mean values. In this example, the two remaining random variables, $K_a$ and $\tan\delta$ are given a negative cross-correlation coefficient of $\rho_{K_a,\tan\delta} = -0.75$ ,on the assumption that a higher soil friction angle will lead to a lower $K_a$ and a higher $\tan\delta$ at the concrete/soil interface below the wall(and vice versa).

This can be set up as a load and resistance problem, where the load ($L$) is the limiting active force and the resistance ($R$) is the maximum mobilized frictional force beneath the wall. Following some arithmetic, it can be shown that $L = 238.71K_a$ and $R = 238.40\tan\delta$. Next it is necessary to set up a performance function $M$ in which $M < 0$ signifies failure (wall sliding). As usual, a choice of performance functions present themselves. One option is to base the performance function on the Factor of Safety, where

$$M = FS - 1 \quad \text{where} \quad FS = \frac{R}{L} = \frac{238.40 \ \tan\delta}{238.71 \ K_a} \tag{5}$$

As an aside, it may be noted that the factor of safety based on means from Table 3 is given by $\overline{FS} = 1.5$

Geotechnical engineers are familiar with the concept of a Factor of Safety, so Eq.(5) may at first seem a good choice, however this performance function is nonlinear with respect to the random variables, since they are represented as a quotient.

As recommended earlier in the paper, FOSM users should look for a performance function that is linear, hence the calculation will continue with

$$M = R - L = 238.40 \ \tan\delta - 238.71 \ K_a \tag{6}$$

From Eqn.(4),

$$\text{Cov}\left[K_a, \tan\delta\right] = -0.75 \times 0.033 \times 0.05 = -0.0012375 \tag{7}$$

and from Eq.(6)

$$\frac{\partial M}{\partial\left(\tan\delta\right)} = 238.40 \quad \text{and} \quad \frac{\partial M}{\partial K_A} = -238.71 \tag{8}$$

hence from Eqs.(3)

$$\begin{aligned} \mu_M &= 238.40 \times 0.5 - 238.71 \times 0.333 = 39.71 \\ \sigma_M &= \sqrt{0.05^2 \times 238.40^2 + 2 \times 0.0012375 \times 238.40 \times 238.71 + 0.033^2 \times 238.71^2} = 18.57 \end{aligned} \tag{9}$$

It then follows that the reliability index is given by

$$\beta = \frac{\mu_M}{\sigma_M} = \frac{39.71}{18.57} = 2.14 \tag{10}$$

and the probability of failure, assuming $M$ is normal, by

$$p_f = 1 - \Phi\left(\beta\right) = 0.016 \ \ (1.6\%) \tag{11}$$

It may be noted that FOSM requires no assumption to be made about the distributions of the input parameters.

Exactly the same result is given by FORM for the same data, which is to be expected since the performance function used in FOSM is linear. If the small variability of the unit weights is included, FORM gives $p_f = 0.017$ (1.7%)

## 3 FORM

The First Order Reliability Method (FORM) typically employs an optimization algorithm that searches systematically for the closest point on the performance function to the mean point of a multi-variate probability density function. The performance function is the locus of $M = 0$. The closest point is often referred to as the "design point", which is an unfortunate choice of words since these values correspond to failure, and would certainly not be used in design. A much better term is the "most likely failure point". Table 2 shows that the FORM solutions are all the same regardless of the arrangement of the Performance Function. The consistent solutions delivered by FORM is an attractive advantage of the method.

Once the most likely failure point has been found, the reliability index follows, as indicated on Figure 5, as the smallest contour value of $\beta$ just touching the performance function. For a normal distribution, the probability of failure can then be found using

$$p_f = 1 - \Phi\left(\beta\right) \tag{12}$$

where $\Phi\left(.\right)$ is the standard normal cumulative distribution function.

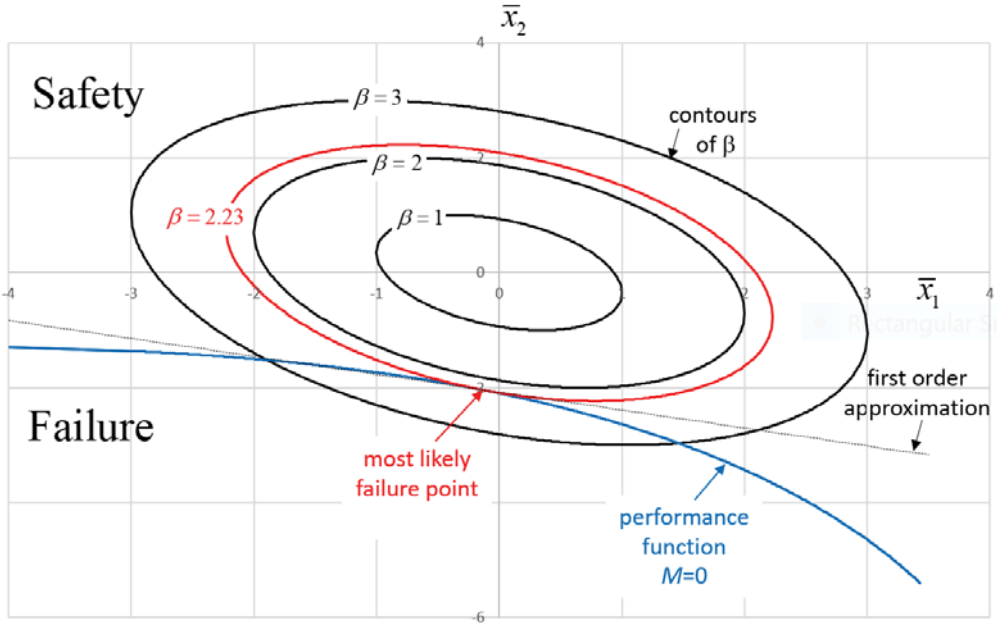


**Figure 5.** FORM finds the most likely failure point and the reliability index

Figure 5 shows a case involving two normal correlated random variables $X_1$ and $X_2$ with parameters $\left(\mu_{x_1}, \sigma_{x_1}\right)$and $\left(\mu_{x_1}, \sigma_{x_1}\right)$, and a correlation coefficient given by $\rho$. In Figure 5, the random variables have been transformed to standard normals, where $\bar{x}_1 = \dfrac{x_1 - \mu_{x_1}}{\sigma_{x_1}}$ and $\bar{x}_2 = \dfrac{x_2 - \mu_{x_2}}{\sigma_{x_2}}$ (Hasofer and Lind 1974) hence the mean point is given by $\bar{x}_1 = 0$ and $\bar{x}_2 = 0$. A conventional FORM analysis using a standard optimization algorithm, will then find the most likely failure point $\left(\bar{x}, \bar{y}\right)_{MLFP}$, and hence the reliability index $\beta$. The method is called "first order" because once $\left(\bar{x}, \bar{y}\right)_{MLFP}$ has been found, the performance function is replaced by a linear function at $\left(\bar{x}, \bar{y}\right)_{MLFP}$ with the same slope, as shown in Figure 5. It can be seen that in this case the first order approximation will lead to a small overestimation of $p_f$.

### 3.1 FORM by solution of nonlinear equations

An alternative to the optimization method for finding the most likely failure point and the reliability index, is to solve simultaneous nonlinear equations using a numerical method such as Newton-Raphson. Consider the following nonlinear performance function (Eq.13) involving two $(n = 2)$ correlated normal random variables $X_1$ and $X_2$ and a second function (Eq.14), representing the contours of the reliability index $\beta$ (Hasofer and Lind 1974).

$$ax_1^3 + bx_2^2 + c = 0 \tag{13}$$

$$\sqrt{\begin{bmatrix} \dfrac{x_1 - \mu_{x_1}}{\sigma_{x_1}} & \dfrac{x_2 - \mu_{x_2}}{\sigma_{x_2}} \end{bmatrix} \begin{bmatrix} 1 & \rho \\ \rho & 1 \end{bmatrix}^{-1} \begin{Bmatrix} \dfrac{x_1 - \mu_{x_1}}{\sigma_{x_1}} \\ \dfrac{x_2 - \mu_{x_2}}{\sigma_{x_2}} \end{Bmatrix}} - \beta = 0 \tag{14}$$

It can be noted that the inverse of the correlation matrix in this case is given by

$$\begin{bmatrix} 1 & \rho \\ \rho & 1 \end{bmatrix}^{-1} = \begin{bmatrix} \dfrac{1}{1-\rho^2} & \dfrac{-\rho}{1-\rho^2} \\ \dfrac{-\rho}{1-\rho^2} & \dfrac{1}{1-\rho^2} \end{bmatrix} = \begin{bmatrix} c_{11} & c_{12} \\ c_{21} & c_{22} \end{bmatrix} \tag{15}$$

which in the interests of simplifying the algebra, will be represented using $c_{ij}$ terms as shown.

Further simplification is achieved by squaring Eq.(14) and expanding the matrix products. Finally, for clarity, the variables $(x_1, x_2)$ are temporarily replaced by $(x, y)$ leading to the pair of equations:

$$ax^3 + by^2 + c = 0 \tag{16}$$

$$\left(\frac{x-\mu_x}{\sigma_x}\right)^2 c_{11} + \left(\frac{x-\mu_x}{\sigma_x}\right)\left(\frac{y-\mu_y}{\sigma_y}\right)(c_{12}+c_{21}) + \left(\frac{y-\mu_y}{\sigma_y}\right)^2 c_{22} - \beta^2 = 0 \tag{17}$$

To find the point of tangency, first compute $\frac{dy}{dx}$ from both Eqs.(16) and (17)and equate them (Martin 2022). Thus from Eq.(16),

$$3ax^2 + 2by\frac{dy}{dx} = 0 \tag{18}$$

hence

$$\frac{dy}{dx} = -\frac{3ax^2}{2by} \tag{19}$$

and from Eq.(17)

$$2\frac{x-\mu_x}{\sigma_x}\frac{1}{\sigma_x}c_{11} + \left[\frac{x-\mu_x}{\sigma_x}\frac{1}{\sigma_y}\frac{dy}{dx} + \frac{y-\mu_y}{\sigma_y}\frac{1}{\sigma_x}\right](c_{12}+c_{21}) + 2\frac{y-\mu_y}{\sigma_y}\frac{1}{\sigma_y}c_{22}\frac{dy}{dx} = 0 \tag{20}$$

which can be rearranged as

$$\frac{dy}{dx}\left[2\frac{y-\mu_y}{\sigma_y}\frac{1}{\sigma_y}c_{22} + \frac{x-\mu_x}{\sigma_x}\frac{1}{\sigma_y}(c_{12}+c_{21})\right] + \left[2\frac{x-\mu_x}{\sigma_x}\frac{1}{\sigma_x}c_{11} + \frac{y-\mu_y}{\sigma_y}\frac{1}{\sigma_x}(c_{12}+c_{21})\right] = 0 \tag{21}$$

hence

$$\frac{dy}{dx} = -\frac{2\frac{x-\mu_x}{\sigma_x}\frac{1}{\sigma_x}c_{11} + \frac{y-\mu_y}{\sigma_y}\frac{1}{\sigma_x}(c_{12}+c_{21})}{2\frac{y-\mu_y}{\sigma_y}\frac{1}{\sigma_y}c_{22} + \frac{x-\mu_x}{\sigma_x}\frac{1}{\sigma_y}(c_{12}+c_{21})} \tag{22}$$

Equating $\frac{dy}{dx}$ from Eqs. (19) and (22) gives

$$-\frac{2\frac{x-\mu_x}{\sigma_x}\frac{1}{\sigma_x}c_{11} + \frac{y-\mu_y}{\sigma_y}\frac{1}{\sigma_x}(c_{12}+c_{21})}{2\frac{y-\mu_y}{\sigma_y}\frac{1}{\sigma_y}c_{22} + \frac{x-\mu_x}{\sigma_x}\frac{1}{\sigma_y}(c_{12}+c_{21})} = -\frac{3ax^2}{2by} \tag{23}$$

Eq.(16) remains unchanged as the performance function, which is now combined with the equated derivatives from Eq.(23) to give the following pair of nonlinear equations.

$$f_1(x,y) = ax^3 + by^2 + c = 0 \tag{24}$$

$$f_2(x,y) = \frac{2\frac{x-\mu_x}{\sigma_x}\frac{1}{\sigma_x}c_{11} + \frac{y-\mu_y}{\sigma_y}\frac{1}{\sigma_x}(c_{12}+c_{21})}{2\frac{y-\mu_y}{\sigma_y}\frac{1}{\sigma_y}c_{22} + \frac{x-\mu_x}{\sigma_x}\frac{1}{\sigma_y}(c_{12}+c_{21})} - \frac{3ax^2}{2by} = 0 \tag{25}$$

Solution of these two equations will give the most likely failure point $(x,y)_{MLFP}$, and hence $(\bar{x}_1, \bar{x}_2)_{MLFP}$.

A Newton-Raphson solution strategy (e.g. Program 3.7 from Griffiths and Smith 2008) will be used which requires further differentiation, so to reduce the volume of algebra, define

$$g(x,y) = 2\frac{x-\mu_x}{\sigma_x}\frac{1}{\sigma_x}c_{11} + \frac{y-\mu_y}{\sigma_y}\frac{1}{\sigma_x}(c_{12}+c_{21}) \tag{26}$$

and

$$h(x,y) = 2\frac{y-\mu_y}{\sigma_y}\frac{1}{\sigma_y}c_{22} + \frac{x-\mu_x}{\sigma_x}\frac{1}{\sigma_y}(c_{12}+c_{21}) \tag{27}$$

hence Eq.(25) becomes

$$f_2(x,y) = \frac{g(x,y)}{h(x,y)} - \frac{3ax^2}{2by} = 0 \tag{28}$$

For Newton-Raphson, further differentiation of Eqs. (24) and (28) gives

$$\begin{aligned} &\frac{\partial f_1}{\partial x} = 3ax^2 && \frac{\partial f_1}{\partial y} = 2by \\ &\frac{\partial f_2}{\partial x} = \frac{2c_{11}h(x,y)\sigma_y - (c_{12}+c_{21})g(x,y)\sigma_x}{\sigma_x^2\sigma_y\left(h(x,y)\right)^2} - \frac{6ax}{2by} && \frac{\partial f_2}{\partial y} = \frac{(c_{12}+c_{21})h(x,y)\sigma_y - 2c_{22}g(x,y)\sigma_x}{\sigma_x\sigma_y^2\left(h(x,y)\right)^2} + \frac{3ax^2}{2by^2} \end{aligned} \tag{29}$$

Consider a particular case with parameters given in Table 4.

**Table 4.** Parameters used in the example problem

| *a* | *b* | *c* | $\mu_x$ | $\sigma_x$ | $\mu_y$ | $\sigma_y$ | $\rho$ |
|---|---|---|---|---|---|---|---|
| -0.01 | -0.3 | 11.0 | 6.0 | 1.0 | 7.0 | 0.75 | -0.35 |

Returning to the subscript notation for the random variables, the initial guess $(x_1, x_2)_0$ used in the Newton-Raphson program, should not be set equal to $(\mu_{x_1}, \mu_{x_2})$, since this will lead to dividing by zero in Eqs.(26) and (27). The results shown in Table 5areobtained with an initial guess of $(6,6)$

**Table 5.** Results file from Program 3.7 (Griffiths and Smith 2008)

```
---Newton-Raphson for Systems of Equations---
          Guessed Starting Vector
             6.0000     6.0000

          First Few Iterations
            5.8917      5.4637
            5.8504      5.5106
            5.8440      5.4770
            5.8442      5.4785
            5.8442      5.4784
            5.8442      5.4784
            5.8442      5.4784
        Iterations to Convergence
                    8

        Most likely failure point
            5.8442      5.4784

                  beta
                2.2294
```

The most likely failure point is given as $(x_1, x_2)_{MLFP} = (5.844, 5.478)$, which after normalization becomes $(\bar{x}_1, \bar{x}_2)_{MLFP} = (-0.155, -2.029)$ as shown in Figure 5. The solution was obtained in 8 iterations with a convergence tolerance of $1\times10^{-8}$. Having found the most likely failure point, the reliability index of $\beta = 2.23$ follows from Eq.(14).

## 4 RFEM

The Random Finite Element Method was developed in the 1990's (Griffiths and Fenton 1993, Fenton and Griffiths 1993, Fenton and Vanmarcke 1990, Smith and Griffiths 2004) for advanced probabilistic analysis in geotechnical engineering. The method involves random field generation of soil properties combined with finite element analysis, with local averaging corrections to account for element size. It is the only method able to account systematically for spatial correlation of soil properties. In addition to the mean (μ) and standard deviation (σ) of soil properties therefore, the RFEM also requires as input the spatial correlation length(θ) which has units of length and may be anisotropic $\left(\theta_x \neq \theta_y\right)$. Source code for 10 geotechnical applications is available for free download as shown in Table 5 below.

**Table 5.** RFEM programs available for free download from `random.engmath.dal.ca/rfem/`

1. mrbear2d: 2-D shallow foundation stochastic bearing capacity analysis,
2. mrdam2d: 2-D stochastic earth dam analysis,
3. mrearth2d: 2-D stochastic earth pressure analysis,
4. mrflow2d: 2-D stochastic seepage analysis,
5. mrflow3d: 3-D stochastic seepage analysis,
6. mrpill2d: 2-D stochastic pillar analysis,
7. mrpill3d: 3-D stochastic pillar analysis,
8. mrsetl2d: 2-D shallow foundation stochastic settlement analysis,
9. mrsetl3d: 3-D shallow foundation stochastic settlement analysis,
10. mrslope2d: 2-D stochastic slope stability analysis,

Due to the great interest in the probability of slope stability failure as an important alternative to the traditional factor of safety, the author and Professor J.

Huang of the University of Newcastle, NSW, have developed an upgraded version of `mrslope2d`. Currently called `twosided`,the enhanced version gives users the option of(i) two-sided embankments,(ii) two soil layers,each with their own statistical properties and (iii) a seepage surface and external reservoir water surface as shown in Figure6. Much research remains to be performed using these enhanced features.

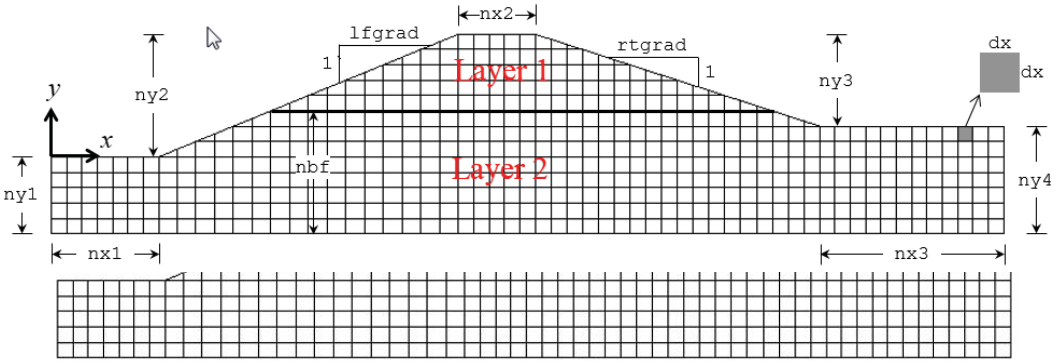


**Figure 6.** RFEM program `twosided`allows a two-sided embankment, two soil layers and a free-surface

### 4.1 Probabilistic analysis of the critical pool level by RFEM

The inclusion of water in `twosided` is an important upgrade, so the first example considered here is a probabilistic analysis of the classical problem of the critical pool level. It has been observed that when a $c'-\phi'$ slope includes a horizontal water table that continues outside the slope as free-standing water, there is a "worst-case" elevation of the water table that leads to a minimum factor of safety (Lane and Griffiths 1997, Griffiths and Lane 1999, Bromhead et al. 1999, Michalowski 2009). Figure 7 shows the basic geometry and a typical random field in which dark zones represent stronger soil.

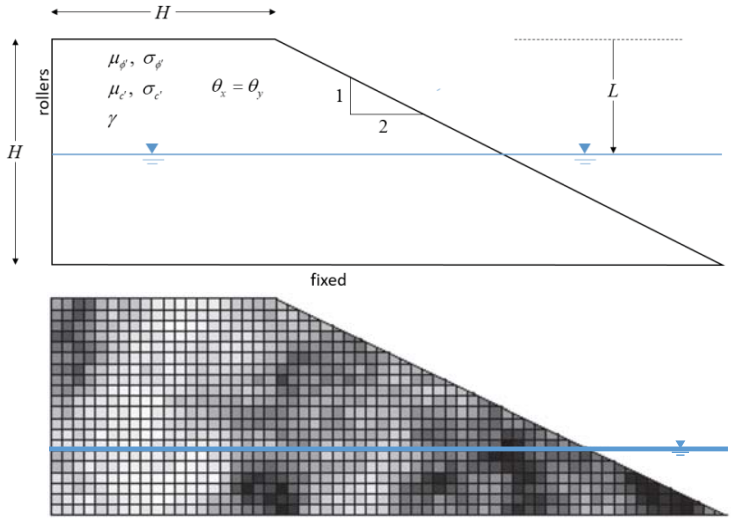


**Figure 7.** Geometry of slope for RFEM probabilistic critical pool analysis and a typical random field of cohesion.

Previous investigations of the critical pool level have been deterministic, so in this study a probabilistic analysis is presented, where the shear strength parameters are random and lognormal. The unit weight of the soil is deterministic, as is the height of the 2:1 slope. The following parameters are assumed:

$\mu_{\phi'} = 20°$, $\sigma_{\phi'}$=4°, $\mu_{c'}$=10 kPa, $\sigma_{c'}$=5 kPa, $\gamma$=20 kN/m$^3$ (above and below WT), $H = 10$ m

The RFEM analyses investigate the probability of slope failure for different depths of the water table below the crest given by $L$. Each value of the water depth in the range $0 \le L \le H$ was investigated using 1000 Monte-Carlo simulations. A fail/no-fail analysis was performed for each simulation, so the probability of failure $p_f$ was estimated as the number of simulations that indicated slope failure divided by 1000. Repeatability checks confirmed that 1000 simulations were sufficient for reasonable accuracy. Three isotropic spatial correlation lengths were considered in the study where $\theta = 2.5, 5.0$ and 10 m.

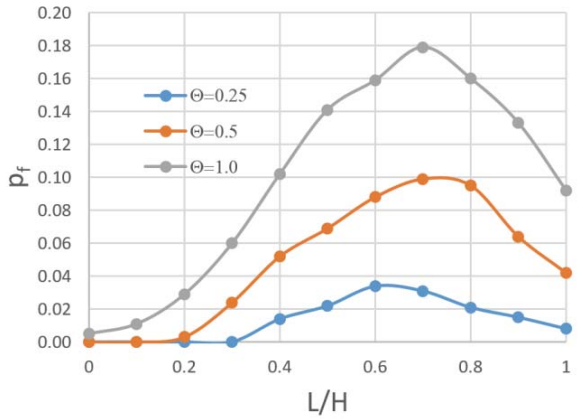


**Figure 8.** Probabilistic critical pool level analysis using RFEM

The results shown in Figure 8 use a dimensionless water depth $(L/H)$ and spatial correlation length $(\Theta = \theta/H)$. All three curves indicate striking $p_f$ maxima in the vicinity of $L/H \approx 0.7$ which agrees with the deterministic results for a minimum factor of safety.The explanation of this phenomenon lies in the trade-off between the stabilizing influence of the free-standing water outside the slope and the de-stabilizing influence of the pore pressures within the slope affecting the frictional component of resistance.

### 4.2 Worst case spatial correlation length in a probabilistic active earth pressure analysis

The "worst case" spatial correlation length is by now a well-known phenomenon in probabilistic geotechnical analysis. Firstnoted by Baecher and Ingra (1981)in a settlement problem and since shown numerically in numerous geotechnical applications using the Random Finite Element Method, e.g. Griffiths and Fenton (1993) in seepage analysis, Fenton and Griffiths (2002) in differential settlement and Zhu et al. (2019) in slope stability analysis.

In this section, the influence of spatial correlation on the active earth pressure acting on a smooth retaining wall is presented, following the work of Fenton et al. (2005), Allahverdizadeh (2015) and Allahverdizadeh et al. (2016). The program used was `mrearth2d` from Table 5. Figure 9 shows the finite element mesh used for the analyses with a wall of height $H = 1\text{m}$.

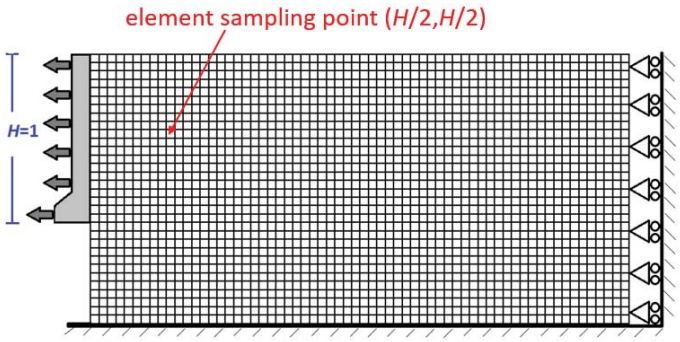


**Figure 9.** Finite element mesh used for probabilistic active earth pressure analysis

The soil was assumed to be cohesionless, with a mean strength of $\mu_{\tan\phi'} = 0.577$ $\left(\mu_{\phi'} \approx 30°\right)$ and a deterministic unit weight of $\gamma = 20\,\text{kN/m}^3$. The coefficient of variation $\left(V = \sigma_{\tan\phi'}/\mu_{\tan\phi'}\right)$ and (isotropic) spatial correlation length $\left(\Theta = \theta/H\right)$of $\tan\phi'$ were then varied in an extensive parametric study. For each combination of $V$ and $\Theta$, a Monte-Carlo simulation involved generation of a random field of $\tan\phi'$, followed by incremental translation of the wall away from the soil until the average limiting active force against the wall fell to a constant minimum value given by $P_{aR}$.

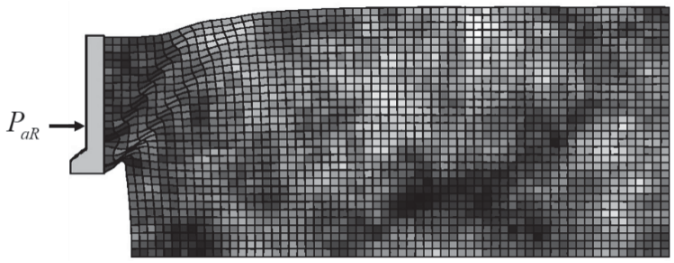


**Figure 10.** Typical simulation of the probabilistic active earth pressure analysis (deformations magnified)

In addition to the above, with each random field simulation, a virtual soil "sample" was taken at a depth and distance from the wall of $H/2$ as indicated in Figure 9. This sampled value, $\tan\phi'_S$ was then used in a Rankine active earth pressure calculation to estimate the active force on the wall given by[2]

$$P_{aS} = \frac{\gamma H^2}{2\left[\tan\phi'_S + \left(1+\tan^2\phi'_S\right)^{1/2}\right]^2} \tag{30}$$

A typical Monte-Carlo analysis involved 1000 simulations, with each giving different values of $P_{aR}$ and $P_{aS}$

The Rankine earth force from Eq.(30) was increased by a Factor of Safety to give a "design" value, which was then compared with $P_{aR}$ from the RFEM analysis. Finally, the probability of failure $p_f$ was defined as

$$p_f = \text{P}\left[P_{aR} > FS \times P_{aS}\right] \tag{31}$$

and estimated as the number of simulations in which $P_{aR} > FS \times P_{aS}$ divided by the total number of simulations performed. Several different values of $FS$ were considered in the study with results shown in Figure 11.

---

[2] Note the identity for $K_a = \tan^2(45° - \phi'/2) \equiv \left[\tan\phi' + \left(1+\tan^2\phi'\right)^{1/2}\right]^{-2}$ (Griffiths et al. 2002)

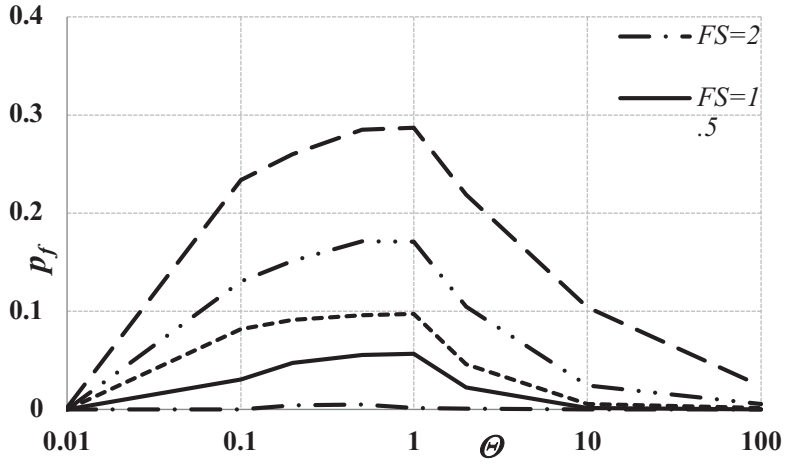


**Figure 11.** Probability of failure vs. spatial correlation length for the active earth pressure problem with different *FS* values, $V = 0.2$ and $\mu_{\tan\phi'} = 0.577$

The most striking features of these results are the very pronounced maxima in the probability of failure for all $FS$-values . With a coefficient of variation of $V = 0.2$, the maxima occurred around $\Theta \approx 1$, however it was noted that for higher values of $V$ (results not shown in this paper), the maxima occurred at lower values of $\Theta$. The results show that there is a "worst case" spatial correlation length giving higher values of $P_{aR}$ from the RFEM analyses. Stability problems such as these are dominated by the weaker soil, and the result suggests that for $V = 0.2$, a spatial correlation length approximately equal to the height of the wall, facilitates the formation of failure mechanisms passing through weaker zones. These weaker zones have lower friction angles leading to higher active forces. Further results from these parametric studies can be found in Allahverdizadeh (2015).

## 5 Concluding Remarks

It is well known that the FOSM method can give non-unique results depending on the way in which the performance function is arranged. This great disadvantage of the FOSM method is tempered by its convenience as a hand computation tool, and the fact that many geotechnical functions exhibit almost linear behavior around the mean values where derivatives are computed. The FORM method on the other hand gives unique results regardless of the arrangement of the performance function. If the performance function is a linear function of the random variables however, FOSM and FORM give the same result. When using the FOSM method therefore, it is important to choose a linear arrangement of the performance function if possible. It may be justified to treat some random variables with relatively small variability as deterministic, if this facilitates a linear combination of the more influential remaining random variables.

The FORM is typically solved as an optimization problem, in which the "most likely" values of the random input variables to cause failure are found using routine software (e.g. Excel). In this paper, an alternative solution method is proposed in which the most likely values are found using a Newton-Raphson algorithm for systems of nonlinear equations. An example was presented to find the point of tangency between a nonlinear performance function and the elliptical contours of the reliability index. The method seems robust, and converged well using freely available software. Interested readers are encouraged to extrapolate this approach to multiple random variables.

The RFEM is a more computationally intensive method that superimposes locally averaged random fields for each input random variable over a refined finite element mesh, followed by Monte-Carlo simulations. The method is the only one that can properly account for the mean, standard deviation *and* spatial correlation structure of a soil deposit. Both the examples presented in this paper led to interesting maxima in the probability of failure as a function of varying conditions.

The first example examined the critical pool level of a $c' - \phi'$ slope subjected to a varying horizontal water table. The results indicated a maximum $p_f$ corresponding to a critical height of the water table at about 30% of the slope height above the base. This is consistent with earlier deterministic studies of this problem, which led to a minimum factor of safety observed at a similar location. The second example showed the influence of spatial correlation length on an active earth pressure problem in which the earth pressure computed by RFEM was compared with a factored deterministic value based on a virtual soil sample taken at a given location. A striking maximum in the probability of failure was observed at a "worst case" correlation length similar to the wall height. In the absence of good quality data on the spatial correlation length at a soil site, the "worst case" spatial correlation length might be initially assumed for conservative design.

Risk assessment of design failure requires an estimate of the probability of failure, weighted by the consequences of failure. The consequences of failure are highly site specific, but the probability of failure can be estimated independently. The paper described three probabilistic tools of increasing complexity, namely FOSM, FORM and RFEM. In all the methods, the goal was essentially the same, namely to estimate the probability of failure, either ultimate or serviceability, depending on the selected performance function. All the methods required the mean and standard deviation of the input random variables, but the RFEM was alone in also requiring information about spatial correlation lengths. The paper aimed to highlight some characteristics and curiosities of results given by the different methods, which might guide users in their proper application to probabilistic geotechnical analysis.

**References**


Allahverdizadeh, P. (2015) Risk assessment and spatial variability in geotechnical stability problems, PhD Thesis, Colorado School of Mines

Allahverdizadeh, P., Griffiths, D.V. and Fenton, G.A. (2016) Influence of soil shear strength spatial variability on the compressive strength of a block. *Georisk,* 10(1), 2-10

Ang, A. H-S. and Tang, W. (2007) Probability Concepts in Engineering: Emphasis on Applications to Civil and Environmental Engineering2nd ed, John Wiley & Sons, Inc.

Baecher, G.B. (2013) Provenance of the Tonen FN chart. Memorandum.

Baecher, G.B., and Ingra, T.S., (1981) Stochastic FEM in settlement predictions. *J Geotech Eng Div, ASCE*, 104(4), 449-463

Baecher, G.B. and Christian, J.T. (2003). *Reliability and Statistics in Geotechnical Engineering*, Wiley, Chichester, U.K.

Bromhead, E.N., Harris, A.J. and Watson, P.D.J. (1999) Influence of pore water pressures in partially submerged slopes on the critical pool level. Proc Slope Stab Eng, (eds. Yagi et al.), Balkema, 411-416

DiMaggio, J.A. (2022) Risk management for infrastructure geotechnical features. On-line lecture given to the Academy of Geotechnical Professionals. March 2022

Duncan, J.M. (2000) Factors of safety and reliability in geotechnical engineering. *J Geotech Geoenviron Eng*, 126(4), 307-316

Fenton, G.A. and Vanmarcke, E.H. (1990) Simulation of random fields via local average subdivision. . *J Eng Mech*, 116(9), 1733-1749

Fenton, G.A. and Griffiths, D.V. (1993) Statistics of block conductivity through a simple bounded stochastic medium. *Water Resour Res*, 29(6), 1825-1830

Fenton, G.A. and Griffiths, D.V. (2002) Probabilistic foundation settlement on spatially random soil. *J Geotech Geoenviron* Eng, 128(5), 381-390

Fenton, G.A., Griffiths, D.V. and Williams, M.B. (2005) Reliability of traditional retaining wall design. *Géotechnique*, 55(1), 55-62

Fenton, G.A. and Griffiths, D.V. (2008) Risk Assessment in Geotechnical Engineering, John Wiley & Sons, Hoboken

Griffiths, D.V. and Fenton, G.A. (1993) Seepage beneath water retaining structures founded on spatially random soil. *Géotechnique*, 43(4), 577-587

Griffiths, D.V. and Lane, P.A. (1999) Slope stability analysis by finite elements. *Géotechnique*, 49(3), 387-403

Griffiths, D.V., Fenton, G.A. and Tveten, D.E. (2002) Probabilistic geotechnical analysis: How difficult does it need to be? Proc Int Conf on *Probabilistics in Geotechnics: Technical and Economic Risk Estimation*, (eds. R. Poettler et al.), Pub. VGE, Essen, Germany, 3-20

Griffiths, D.V. and Smith, I.M. (2008) Numerical Methods for Engineers, Chapman & Hall/CRC, 2nd ed., Boca Raton

Hasofer, A.M. and Lind, N.C. (1974) Exact and invariant second-moment code format.*J. Eng Mech, ASCE*, 100, 111–121.

Huang, J. and Griffiths, D.V. Observations on FORM in a simple geomechanics example. *Struct Safety*, 33(1), 115-119

Lambe T.W. & Associates (1982) *Acceptable risk at Kawasaki site 400.* Report prepared for Towa NenryoKogyo Co. Ltd. (now TONEN Corporation), Kawasaki, Japan, by G.B. Baecher and W.A. Marr, Cambridge, MA

Lane, P.A. and Griffiths, D.V. (1997) Finite element slope stability—Why are engineers still drawing circles? Proc NUMOG VI, (eds. G.N. Pande and S. Pietruszczak), Montreal, Balkema, pp.589-593

Lee, I.K., White, W. and Ingles, O.G. (1983) Geotechnical Engineering, Pitman, Boston

Low, B.K. and Tang, W. (1997) Efficient reliability evaluation using spreadsheet, *J Eng Mech, ASCE*, July, pp 749-752

Low, B.K. and Tang, W. (2007) Efficient spreadsheetalgorithm for first-order reliability method,*J Eng Mech, ASCE*, December, pp 1378-1387

Martin, P.A. (2022) Colorado School of Mines, Private communication.

Meyerhof, G.G. (1963). Some recent research on the bearing capacity of foundations. *Canadian Geotechnical Journal*, 1(1), 16-26.

Michalowski, R.L. (2009) Critical pool level and stability of slopes in granular soils. *J Geotech Geoenviron Eng*, 135(3), 444-448

Schiermeyer, R.P. (2009) Probabilistic methods applied to slopes and footings, MS Thesis, Colorado School of Mines

Smith, I.M. and Griffiths, D.V. (2004) Programming the Finite Element Method, 4th ed., John Wiley & Sons, Chichester

Whitman, R.V. (1984) Evaluating the calculated risk in geotechnical engineering. *J Geotech Eng Div, ASCE*, 110(2), 145-188

Zhu, D., Griffiths, D.V. and Fenton, G.A. (2019) Worst case correlation length in probabilistic slope stability analysis. *Géotechnique*, vol.69, no.1, pp.85-88